Constant Hue Bands in Boundary Colors Discovered Using a New Appearance Model

Louis W. Adams Jr.,[1] Carl Jennings[2]*

[1]155 Chandler Downs Trail, Inman, SC 29349

[2]University of Hawai'i at Kapi'olani, 4303 Diamond Head Road, Honolulu, HI 96816

Received 16 June 2013; revised 8 December 2013; accepted 11 December 2013

Abstract: Boundary colors are observed when light from a scene is dispersed by a prism or diffraction grating. We discovered that patterns with repeating black and white stripes can produce repeating bands of boundary colors with two hues. These hues are virtually constant as measured by chromaticity or CIELAB. We found seven cases of this kind using a new appearance model for boundary colors. The model correctly predicts that green and magenta bands recur as stripe widths and dispersion strength vary. The first green/magenta case in the sequence traces out an accurate ellipse in XYZ color space. Green and magenta bands are prominent in supernumerary rainbows and interference rings, and we explain why that might be the case. The explanation is based on an interesting property of the visible spectrum. In addition to the green/magenta cases, the other cases are orange/cyan, yellowish-green/purple, and yellow/violet. The success of the boundary color appearance model implies that bands are perceived as if the wavelength responses of the cones were essentially independent, which contradicts the actual behavior of cones. © 2014 Wiley Periodicals, Inc. Col Res Appl, 40, 135–146, 2015; Published Online 23 January 2014 in Wiley Online Library (wileyonlinelibrary.com). DOI 10.1002/col.21871

Key words: appearance; boundary colors; categorical perception; color theory; edge spectra; fringe colors; hue; visible spectrum

BACKGROUND

The colorimetry of boundary colors for simple shapes is well understood.[1,2] The simplest special case is the visual spectrum formed by passing white light through a narrow slit that is dispersed by a prism or diffraction grating (dispersing optics). Widening this slit produces boundary colors studied in detail by Newton,[3,4] although he only discusses them very briefly in his *Opticks*.[4 (p 551f),5] Similar images are produced by viewing white rectangles on black backgrounds through dispersing optics. Goethe generalized this method to include black stripes on white backgrounds, and more complex patterns.[6] This includes patterns that are colored. Boundary colors are no longer an active research topic in color science, although Koenderink believes that they could play a fundamental role in a rigorous scientific theory of colorimetry (Ref. 2).

Boundary colors can be visually discrete. When that is the case, then they are perceived as bands of color, each band having constant perceived hue even though colorimetric hue varies as measured using chromaticity or CIELAB. Transitions between perceived hues are relatively abrupt. Psychologists call this categorical perception: continuously changing stimuli are perceived as discrete unchanging categories. (See Shepard[7] for a general discussion about the categorical perception of color.) When the visible spectrum subtends an angle of about 10° in the visual field, then wide (red, green, and violet) and narrow (yellow and cyan) bands are seen. At much smaller angular extensions only red, green, and violet bands are apparent. When viewed at sufficiently wide angular extensions (high magnification) the spectrum then appears to be a hue continuum, and no bands are seen. For example, there is an absence of banding when a solar spectrum is projected onto a large screen, and portions of the spectrum are viewed at a close distance. In summary, the perception of visually discrete bands in boundary colors usually depends on viewing conditions. This report presents special cases where discrete bands are always perceived, and are measurably discrete: both perceived hue and colorimetric hue are constant.

*Correspondence to: Carl Jennings (e-mail: cjenning@hawaii.edu)

Other than Kidder,[8] we cannot cite studies with quantitative analyses of perceived bands, either in the visible spectrum or for boundary colors generally. Ostwald for example comments on the relatively dull appearance of yellow in the visible spectrum,[9] but this is by way of introducing his important ideas on related and unrelated colors, and optimal colors. He does not discuss the width of the yellow band in the spectrum. Kidder analyzed the appearance of the yellow band in the visible spectrum using a neural model, although he did not explicitly address its perceived width.

Our report features repeating boundary colors with two hues, hues that are complementary. Because they arise out of the dispersion of white light this might suggest that the concepts of optimal or ideal colors are relevant, in particular Ostwald's semichromes. However, in our case the colors comprising each band are not optimal or ideal. That is, they are not due to a partition of the Ostwald color circle into halves; white content is high in the colors of both bands. For the pattern of black and white repeating stripes discussed in this report, a boundary color consists of a sum of discrete sections of the visible spectrum. The perception of bands is an appearance phenomenon, and the colorimetry of individual colors in a band is therefore beside the point: each color in a band generally has a different colorimetry (different wavelength composition and different colorimetric hue), yet the colors comprising each band have essentially the same perceived hue.

INTRODUCTION

One way to think of our appearance model is that it simplifies how the visual system responds to light. If the wavelength response curves of the LMS cones in the retina did not overlap, then the visible spectrum would be perceived as consisting of three distinct bands, each band seen as a single hue (red, green, and violet). The spectrum image would therefore be divided approximately into thirds. Any wavelength gap between response curves, where no cone responds, would cause a gap in the perception of the visible spectrum (a dark band separating light ones). If these hypothetical LMS response curves move towards each other so that they begin to overlap, then these overlaps would be perceived as narrow bands with new hues (yellow and cyan). Our appearance model simulates the scenario where the response curves meet without overlapping.

It is well known that the actual LMS response curves are of course not so neatly arranged as assumed by the model. Figure 1 shows the LMS responsivity curves,[10] and the eight principal hues that are usually associated with wavelengths.[11] The S cone response has only a relatively small overlap with the M and L cone responses, which perhaps explains the wide violet band V that is perceived in the visual spectrum. However, the M and L cone responses overlap to a great extent. One naïvely expects the peak response of the L cone to be associated

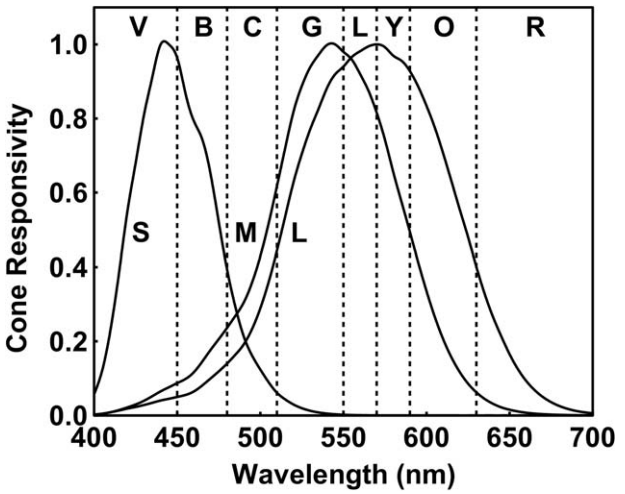

Fig. 1. Responsivity curves for the S, M, and L cones of the retina. Vertical dashed lines show how the visible spectrum is divided into hues associated with spectrum wavelengths.

with a wavelength that is perceived as "red", but that is not true. The perception of red R is perhaps associated with the long-wavelength tail of the L cone, along with a portion of the M cone tail. Based on the L and M curves, the division of the perceived spectrum into green, lime, yellow, orange, and red hues (G, L, Y, and O) seems almost arbitrary. And why is blue B perceived between violet V and cyan C?

It is not possible to understand the perception of the visible spectrum solely from LMS response curves, and this is also well known.[12] In this study we do not investigate the difficult questions posed in the previous paragraph, which become even more complex as viewing conditions change. Our boundary color appearance model nonetheless makes the simplifying assumption that the visual system acts as if the wavelength responses of LMS cones do not overlap and that the rest of the visual system is irrelevant.

The appropriate interpretation of the red, green, and blue color components in our appearance model is that they describe the perception arising out of the stimulus of wavelength mixtures comprising boundary colors. Different combinations of these three components correlate with an observer's perception of six hues: red, yellow, green, cyan, blue, and magenta. Black is perceived as the absence of the three color components, and white is perceived as the presence of all three components. Our appearance model therefore provides a phenomenological mechanism for the categorical perception of boundary colors that arises out of trichromacy. As we shall see, the mechanism is consistent with how band widths change as dispersion or pattern features change.

Symbolically, in our appearance model a band is perceived as a single color Q with R, G, and B color components: Q = (R, G, B). Values for color components can be thought of as 0 or 1; that is, "not present" or "present", respectively. The perceived colors red R, green G, and

yellow Y have components R = (1, 0, 0), G = (0, 1, 0), Y = R + G = (1, 1, 0). Similarly for the other three hues of the appearance model (cyan C, blue B, and magenta M), with black K = (0, 0, 0) and white W = R + G + B = (1, 1, 1). Although this resembles the well-known ideal additive mixing of color primaries, that similarity is misleading. In the appearance model the components refer to aspects of color perception, not physical aspects of the stimulus. The components do not define a color space or other metric. They are categorical and descriptive only.

Color components are part of the output of the appearance model, and we sometimes refer to them as describing the "content" of a color. So the red component of a color specifies the red content of the color. Whether the symbol R represents a color component or a perceived color in this report depends on context. The red color R has a single non-zero color component R, so for all practical purposes the perceived color red is equivalent to the red color component. Yellow is perceived when its color content has both red and green components, but the red and green content of yellow are not perceived. Therefore color components are perceived as colors in isolation, but not when they are in combination with other color components. For this reason it is not appropriate to call the color components the "attributes" of a color because that word is restricted to aspects of a color that are perceived. These distinctions might seem like pedantry, but our model is phenomenological and we cannot ascribe well-defined physical or biological attributes to the model output. As we shall see, this does not prevent the model from being useful and even semi-quantitative.

Besides providing another way of investigating boundary colors, there is a practical reason for using our appearance model. Analyzing the continuum of shifting hues in the colorimetry of boundary colors is much more difficult than keeping track of only 8 colors in bands with definite widths that vary in a simple way. That is, the model makes it easier to understand the appearance of boundary colors as the stimulus varies because the predictions themselves are simplified.

During work to verify that the model correctly predicts the usual boundary colors, we discovered one case where CIELAB hue angle h_{ab} is virtually constant for each boundary color. This occurs for boundary colors produced by a pattern of repeating black and white stripes. The discovery prompted us to use our appearance model and CIE calculations to search for similar cases. After investigating over 60 cases, we found 7 instances of this kind. Four cases are green and magenta bands in a family predicted by our appearance model. Graphing the boundary colors that are calculated from CIE data for the first member of this green/magenta family produces an accurate ellipse in XYZ color space, which reveals a new simple symmetry in the visual system. Such a graph is very irregular when more than two boundary color hues are perceived, which is well known. We believe these discoveries are not previously reported in the color science literature, and that they would likely not have been made without our appearance model.

A SIMPLE EXAMPLE USING THE APPEARANCE MODEL

Before discussing our appearance model in detail for an infinite number of black and white stripes, we present a simpler case to demonstrate the model and its utility. In this example the model is used as a tool to design a black and white pattern. The intended purpose of the pattern is to produce boundary colors that are perceived to contain equal-width bands of all primary (red, green, blue) and secondary (yellow, magenta, cyan) hues. Sketching out possibilities on paper using our model as a guide, we found that one solution is a pattern with a white stripe 1 unit wide, followed by a black stripe 1 unit wide, and followed by a white stripe 2 units wide, all stripes on a black background. There is a 1 unit shift in the color components caused by dispersion.

The appearance model view of the situation is illustrated in Fig. 2(b), the bottom half of the figure. The three color components corresponding to the perception of the dispersed pattern (labeled R, G, B in three rows) are horizontally offset due to dispersion. The color components of the 1 unit wide white stripe on the left are nearly completely separated, while the color components of the 2 unit wide white stripe on the right have 50% overlaps. The output of the appearance model predicts 3 colors that contain only one color component (R, G, and B), and 3 colors with two color components (C, M, and Y), in the sequence shown. The boundary color bands are predicted to have equal widths.

Figure 2(a), the top half of the figure, shows a gamut-mapped sRGB image of the boundary colors calculated using CIE data.[13] Pattern stripe widths were optimized for hue uniformity using trial and error, and a hue classifier (utilizing CIELAB hue angle). Band hues and hue sequence were correctly anticipated by the appearance model. Equally-spaced vertical dashed lines show how the bands in the image line up with the predicted bands at the bottom of the figure. Optimal widths for the narrow black and white pattern stripes in the CIE calculation were found to be equal, as predicted by the model. Although our appearance model predicts that a wide-to-narrow stripe width ratio of 2.0 produces the desired boundary colors, we find that a ratio of 2.5 is necessary to achieve the most uniform hues in the CIE calculation. This result is not indicated in Fig. 2, which depicts how the 2.0 stripe width ratio for the appearance model shown at the bottom correlates with the CIE image based on the 2.5 ratio that is shown at the top.

The leftmost band in Fig. 2(a) is labeled V for violet because that is the hue in the CIE image. That is also how it appears when the boundary colors are observed using a diffraction grating or prism. Our appearance model produces no violet hue, a deficiency of the model. The hue that corresponds to V in the appearance model is

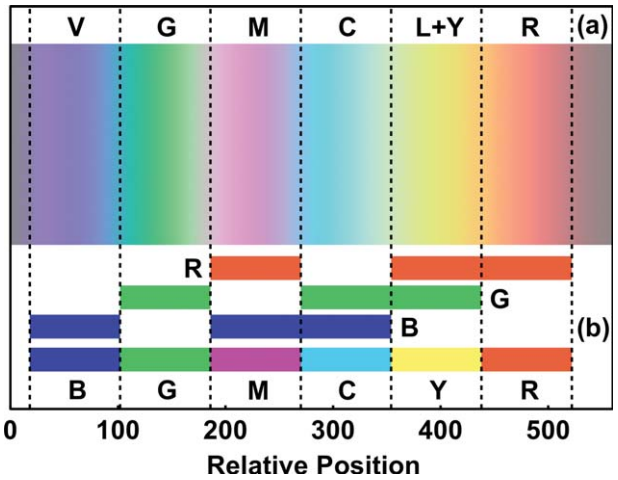

Fig. 2. (a) Equally spaced vertical dashed lines show approximate boundaries between six bands perceived in an image from a CIE calculation. Letters at the top indicate perceived band hues. The pattern generating the boundary colors has two white stripes of different widths surrounded by black. (b) An appearance model for the CIE calculation image. Horizontal bars represent the dispersion displaced color components red R, green G, blue B for the black and white pattern. The six resulting model bands are shown at the bottom, which correspond to the bands in the CIE image at the top of the figure.

labeled B for blue in Fig. 2(b). In this investigation we sometimes find that blue B in the appearance model corresponds to violet V in the CIE calculation. However, blue does appear in boundary colors. For example, an unlabeled narrow blue band lies under the dashed line separating the V and G bands in Fig. 2(a).

There is also a narrow orange band under the dashed line separating the L+Y and R bands. The other boundaries between bands are relatively neutral in color. The white color of the wide white stripe in the pattern nearly peeks through the boundary between the C and L+Y bands.

The yellow band predicted by the appearance model [Fig. 2(b)] is observed in the actual boundary color [Fig. 2(a)] to have a large component of yellowish-green L ("lime"), especially on the left side of the band. This is why the band is labeled L + Y. We find that this is common for "yellow" bands in boundary colors.

The black and white stripe pattern was printed on paper using a 2.5 ratio for the two white stripes, and we viewed the pattern through prisms and diffraction gratings with daylight illumination. Our observations were satisfactory matches to the image in Fig. 2(a). The major difference between the calculated image and the boundary colors is that the observed boundary between the red R and yellow L+Y bands is less distinct than seen in the image in Fig. 1(a). These two bands are also observed to be somewhat wider than the other four. It is possible that adjusting stripe widths on the printed pattern would produce a better match to the desired image. Or it might be necessary to independently adjust the relative stripe widths to achieve the most visually uniform hues. Note that we optimized the CIE based image using a colorimetric measure for hue, not the perceived hue. It is possible that a fully visual means of optimization produces a stripe width ratio that is closer to what our appearance model predicts.

Our calculation of images using CIE data assumes that the dispersion of light is linear with wavelength, which best matches the behavior of diffraction gratings. Prisms are less linear in this regard.

One might ask what happens in Fig. 2(b) when dispersion is further increased and the RGB components of the narrow white stripe fully separate, and gaps form between them. The answer is that strictly speaking this exceeds the range of validity of the appearance model. The spectrum of a continuous light source has, by definition, no gaps between wavelengths, regardless of dispersion level. Therefore a little common sense must be used when applying the model. In what follows we flagrantly break this rule to study boundary colors for large relative dispersions.

THE APPEARANCE MODEL FOR REPEATING BLACK AND WHITE STRIPES

Model Details

Figure 3 illustrates the model for repeating black K and white W stripes shown at the top of the figure. The black and white stripes extend perpendicularly through the plane of the figure, towards and away from the viewer; that is, the figure shows a cross-section of the stripes in the fourth row. Only two stripes are shown, white W and black K, but this pattern is repeated to infinity in the left and right directions. The top three rows show the color components red R, green G, and blue B for the white and black stripes. This is a representation of the situation when there is no dispersion of light in the stimulus: the R, G, and B image components are vertically aligned in the figure. Black bars in the top three rows indicate the absence of color components in the black stripe.

The appearance model has information about the stimulus as its input: a black and white pattern of repeating stripes, and a dispersion displacement parameter x that is proportional to the shift in wavelengths caused by dispersion. The model output is information about the visual system's response to the stimulus: the 6 hues of boundary colors plus black and white, and the widths of these bands expressed in terms of x.

The appearance model assumes that the wavelength shift in the stimulus due to dispersion causes proportionate shifts in the color content of the boundary colors. Relative displacement x is the distance that the red component is shifted towards the right in Fig. 3 due to dispersion. It is equal to the distance that the blue component is shifted simultaneously towards the left. This symmetry means we assume that these shifts are linear both in the stimulus and the response. The perceived width of one white stripe is therefore increased by $2{\cdot}x$ units

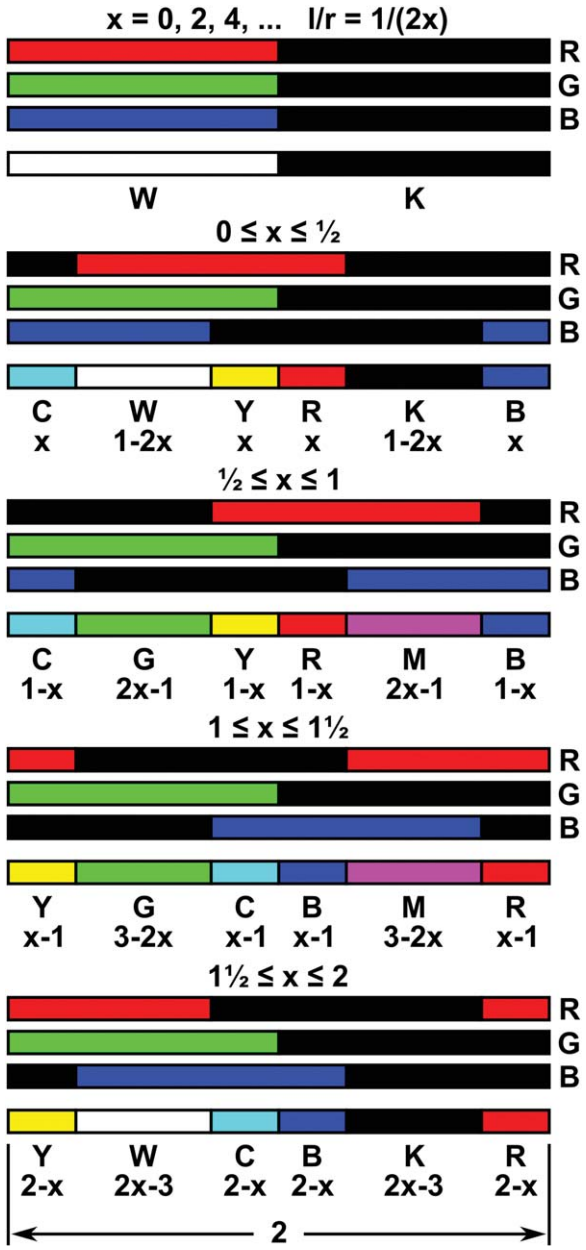

Fig. 3. The appearance model for an infinitely repeating pattern of white stripes 1 unit wide alternating with black stripes 1 unit wide. Only one repeat is shown, with the initial white W and black K stripes shown at the top. The dispersion displacement between the green component and the red and blue components is x, which is 0 at the top and increases down the figure. The resulting band hues (C, W, Y, and so on) and widths (expressed in terms of x) are predictions of the appearance model.

because of dispersion, and the appearance of the stripe is no longer uniformly white; color fringes appear along its edges as seen in row 8 of the figure, in the second group of four rows where $0 \leq x \leq 1/2$. In this model the warm fringes are red and yellow, and the cool fringes are cyan and blue.

The green component is in a reference position and does not shift in Fig. 3 as x changes. In reality all components shift position due to refraction or diffraction. Measuring displacement relative to the green component is a simplifying frame of reference.

Figure 3 uses a fixed pattern scale (two 1 unit wide stripes that repeat). Relative color component displacement x increases down the figure, and the color components move further apart. Boundary colors appear and disappear as illustrated. Bands with colors C, W, Y, R, K, and B occur when x is less than $1/2$. As x increases further, W and K disappear and G and M take their places, respectively. When x equals 1, then the only remaining bands are G and M. As x increases further, bands Y, C, B, and R reappear in new positions, and widen at the expense of G and M. When x equals 2 then the color components have shifted one full pattern repeat: the model predicts that boundary colors return to the initial black and white pattern. (This does not actually happen for boundary colors, as we discuss below.)

These changes are summarized in Fig. 4 where relative band widths are graphed as a function of x for 0 through 1. At each value of x the sum of all relative spatial band widths equals 1. Band widths for colors R, Y, B, and C are always equal, as are G and M, and W and K. Therefore the graph only requires three curves, as indicated by the legend.

The graph labels three cases of curve crossings, marked by vertical dashed lines. For example, when $x = 2/3$, then 6 of the bands are predicted to have equal widths. The G and M bands are absent. Widths in the graph are based on the relationships shown in Fig. 3, which also establishes the sequence of colors. Hue sequence is not apparent in Fig. 4.

When x begins to exceed 1, then the graph in Fig. 4 is read from right to left. The value at $x = 0$ shown on the graph then next corresponds to $x = 2$. In the range of x from n to $n + 1$, where n is an even integer (including $n = 0$), then relative band widths are found by reading the

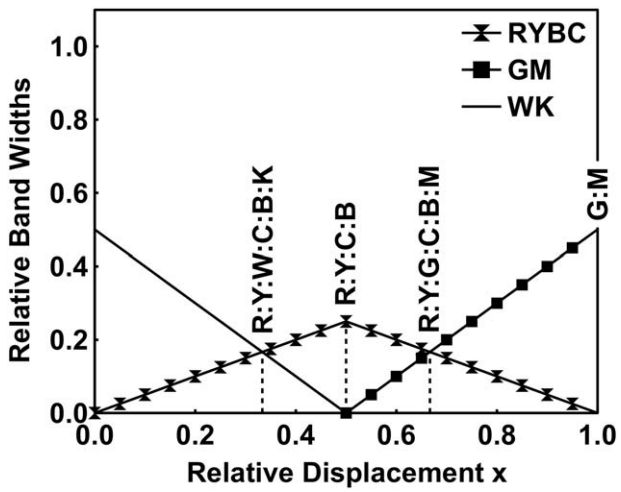

Fig. 4. Relative band widths for the appearance model in Fig. 3. Letters indicate perceived band hues. Four cases are labeled where all boundary color bands have equal widths. This occurs when x equals $1/3$, $1/2$, $2/3$, and 1. The text explains how to use the graph for $x > 1$.

TABLE I. GM cases.

X	$W \pm \Delta W$	$\Delta W/W$
1.0	71 ± 1	1.4%
3.0	25 ± 1	4.0%
5.0	18 ± 1	5.6%
7.0	10 ± 1	10.0%

graph from left to right as x increases. In the range of x from n to $n+1$, where n is odd, then the graph is read from right to left as x increases. In both cases n is the leftmost x value on the graph, and $n+1$ is the rightmost value. For example, $x = 5\frac{1}{3}$ corresponds to the location labeled R:Y:G:C:B:M on the graph (6 bands with equal widths, $16\frac{2}{3}\%$). In this way the graph predicts relative band widths for arbitrarily large values of the dispersion displacement parameter x. In summary, the model predicts that as x increases the boundary colors cycle through a fixed sequence of colors indefinitely.

RESULTS AND ANALYSIS

Green and Magenta Constant-Hue Bands

Figure 4 shows that our appearance model predicts that the first four green and magenta (GM) images occur when x equals 1, 3, 5, and 7. Using CIE calculations (2° Observer and Illuminant D65, wavelengths 400 nm to 700 nm in increments of 1 nm) we find corresponding GM images for stripe widths W equal to 71, 25, 18, and 10 units, respectively. Table I summarizes our data for the GM family. GM boundary colors that might exist for stripe widths smaller than 10 could not be identified because our CIE calculation has insufficient resolution. (The visible spectrum occurs for $W = 1$, and the white and black stripe colors peek through the dispersed colors when $W > 300$. W is always an integer, and dispersion displacement is fixed in our CIE calculations. Only stripe width varies.)

A remarkable feature of the GM boundary colors are their colorimetric hues. Figure 5 shows CIELAB hue angle variation for the first case in the series, $x = 1$ ($W = 71$). The graph shows that both G and M bands have essentially constant hue angles. There are abrupt hue transitions between bands where chroma C^*_{ab} drops to zero; that is, very narrow gray regions separate the bands. Lightness L^* varies sinusoidally, and is out of phase with band boundaries. (The hue angle h_{ab} curve in Fig. 5 is normalized by the factor 360. The L^* and C^*_{ab} curves are normalized so that their maximum values equal 1. Prior to computing CIELAB values, the XYZ values were normalized with respect to the illuminant. These normalizations are used for similar graphs in this report.)

Chromaticity curves (1931) for all four GM cases are compared in Fig. 6. The first number in each curve label is the stripe width W used in the CIE calculation. The low contrast of the images with the three smallest stripe widths would cause the actual chromaticity curves for these cases to graph as points. Therefore the curves were scaled up to make their shapes apparent. For example, it was necessary to scale up the $W = 10$ curve 180 times, so the graph label for this case includes "180x". The scale factors used for the figure are otherwise arbitrary.

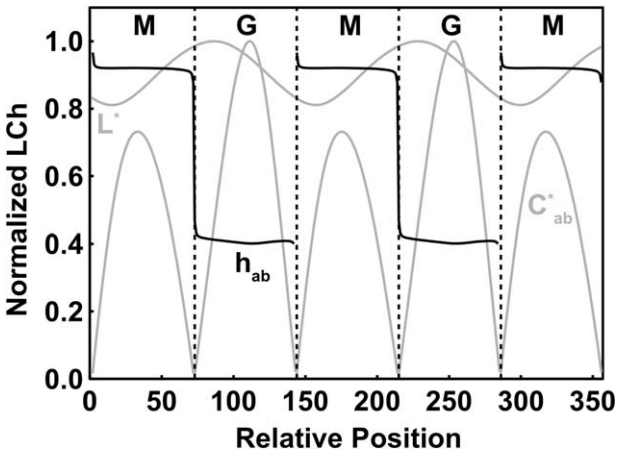

Fig. 5. CIELAB curves for GM ($x = 1$).

The chromaticity curve for $W = 71$ units in Fig. 6 is virtually a straight line through Illuminant D65. This shows that the green and magenta band colors are exactly complementary in colorimetric hue. The bands in each subsequent case have less constant hue, which is apparent from decreasing curve eccentricities. The final case, where $W = 10$ units, has the least constant hue, although eccentricity remains significant. The longest axis of the curves rotate clockwise in the sequence from widest to narrowest stripes, which shows that green bands becomes more yellowish, and magenta bands becomes more bluish (with one exception, discussed next).

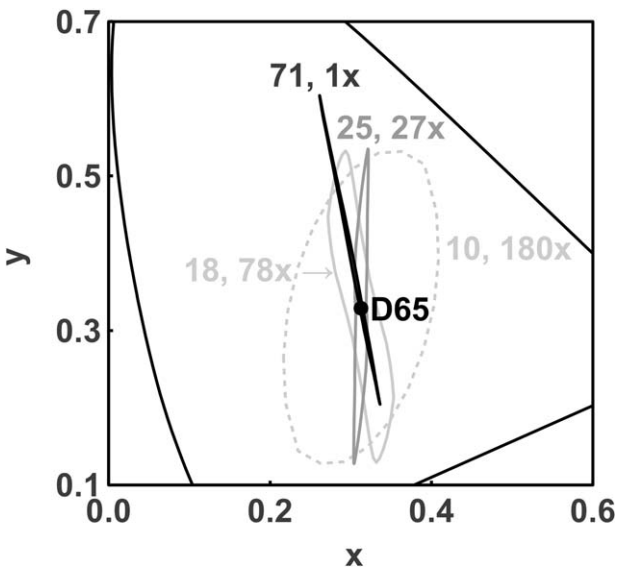

Fig. 6. Chromaticity diagram (1931) for the four GM cases. The first number in each label is the stripe width used in the CIE calculation. The second number is the scaling factor used to magnify the chromaticity curve to make it visible on the diagram.

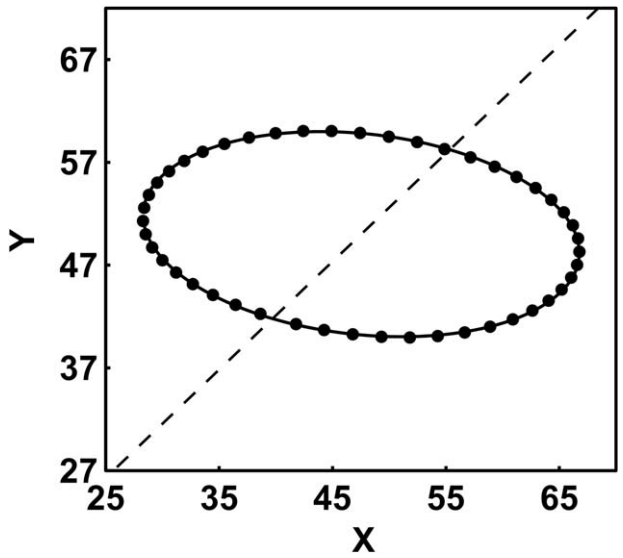

Fig. 7. Tristimulus values X and Y (1931) graphed for GM where $x = 1$. Filled circles are a sample of data points. The solid line passing through the data points is the least squares fit of an ellipse to all data points. The dashed line is the axis of neutral colors, which crosses the ellipse in two places and indicates the boundaries between bands.

Note that $W = 18$ has less constant hue (a larger relative area and smaller eccentricity) than the cases preceding and following it (widths 71 and 25, respectively). It is also rotated counterclockwise from the previous case. This suggests that it is a suboptimal image. The smaller the stripe width, the less likely that an image is optimal for hue constancy. This is because changing stripe widths by 1 unit causes greater image changes as stripe widths become narrower. A more complex CIE calculation incorporating interpolation to increase resolution could resolve whether or not the image for $W = 18$ is optimal for hue constancy; the optimal width lies between 17 and 19 in our calculations.

Because the chromaticity curve for GM with $W = 71$ is a straight line crossing the illuminant point, in tristimulus XYZ color space the data form a curve on a plane that intersects the neutral axis. The curve is the accurate ellipse shown in Fig. 7, a graph of tristimulus values X versus Y (The idea to graph the data in XYZ color space arose during discussions with Dr. Michael H. Brill, Datacolor). The long axis of the ellipse is slightly tilted clockwise from horizontal. The dashed line is the neutral axis (gray line). It intersects the ellipse in two places, at the boundaries between the green and magenta stripes, and thereby divides the ellipse into halves. The right half of the ellipse is data for the magenta band, and the left half is for the green band.

CIE computed boundary colors in Fig. 7 are shown as filled circles, but only 47 of 143 data points are plotted so that the fitted ellipse is not obscured. The solid curve is an ellipse fitted to all 143 points. Deviations from a perfect ellipse do not exceed $\frac{1}{2}$ tristimulus unit in this XY-plane projection; the root mean square error for all of the points is 0.14 for Y values. The view in Fig. 7 is not perpendicular to the plane of the ellipse in XYZ color space. When viewed perpendicularly to that plane, the ellipse is much more elongated than shown in Fig. 7.

TABLE II. OC, LP, and YV cases.

Case	$x \pm \Delta x$	$\Delta x/x$	$W \pm \Delta W$	$\Delta W/W$
OC	1.5 ± 0.1	6.7%	48 ± 1	2.1%
LP	2.0 ± 0.1	5.0%	36 ± 1	2.8%
YV	5.3 ± 0.1	1.9%	16 ± 1	6.3%

Such markedly regular behavior exhibited by the colorimetry for this case of boundary colors leads us to suspect that there must be a special condition that causes the precise elliptical shape. Boundary color trajectories in XYZ color space are usually irregular and do not lie in a plane. It is likely that the condition could be expressed as a special symmetry of the vision system. We performed an analytical integration for the continuum version of the CIE calculation using symbolic algebra software. Color matching functions were approximated by sections of sine curves for the integration. We did not find a condition that determines when trajectories are planar or elliptical. This is a problem for future research.

Three More Cases of Constant-Hue Bands

The only cases of boundary colors with two hues predicted by our appearance model in Fig. 4 are the GM cases discussed in the previous section. Three other cases of this type were found by computing and inspecting all boundary color cases for stripe widths W less than 65 units. (Images were computed in sRGB color space for inspection on a calibrated color display.) Although we did not calculate CIELAB hue curves for all of these images, the appearance of these images suggested to us that only the two-hue boundary color images were likely candidates for hue-constant bands. The new cases are orange and blue-green (OC), yellowish-green ("lime") and purple (LP), and yellow and violet (YV), in that order. Table II summarizes data for these three cases. Figures 8–10 show CIELAB hue angle graphs for the three cases. Like the

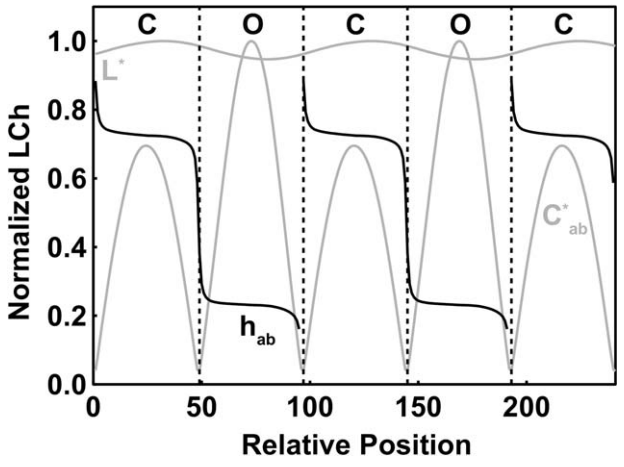

Fig. 8. CIELAB curves for orange/blue-green bands (OC).

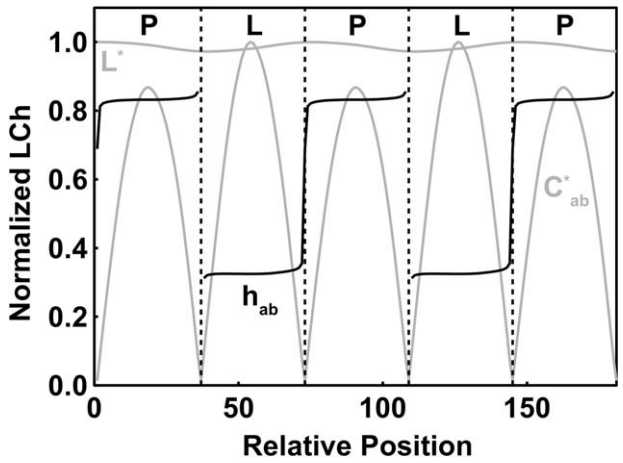

Fig. 9. CIELAB curves for yellow-green/red-violet bands (LP).

GM cases, these new cases exhibit bands with uniform hues and abrupt hue transitions between bands. The sinusoidal L^* curves in this sequence of graphs become shallower as W decreases because contrast decreases.

Figure 11 compares chromaticity curves (1931) for the new cases plus the case GM for $x = 1$ for comparison. As in Fig. 6, chromaticity curves in Fig. 11 are scaled up to make their shapes apparent. The YV case is scaled up by a factor of 95. But even for YV (the case with the narrowest stripe widths in the figure), colorimetric hue is remarkably constant, although the curve has a slight "S" twist.

Our appearance model predicts precise x values for the GM family of boundary colors. However, the three new cases are not explicitly predicted by the model. Nonetheless, values for x for these three cases were estimated by visually correlating our appearance model predictions and CIE calculation sRGB images. Examples of such matches are shown in Fig. 12. Appearance model images are shown on the left, and the closest matching CIE calculation images (contrast enhanced) are shown on the right. Image matching was done by visual assessment. Because of the relative imprecision of the visual matching process,

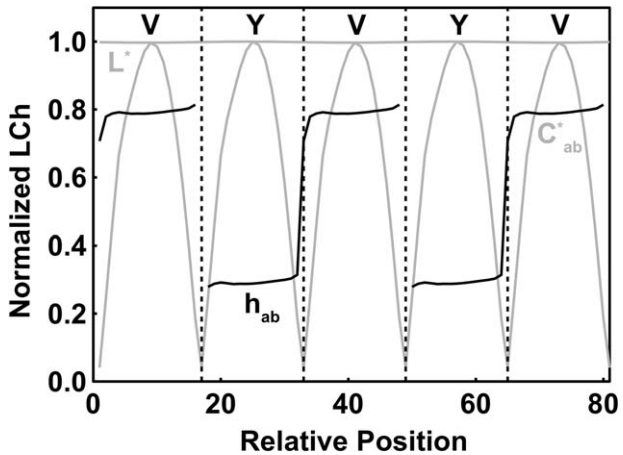

Fig. 10. CIELAB curves for yellow/violet bands (YV).

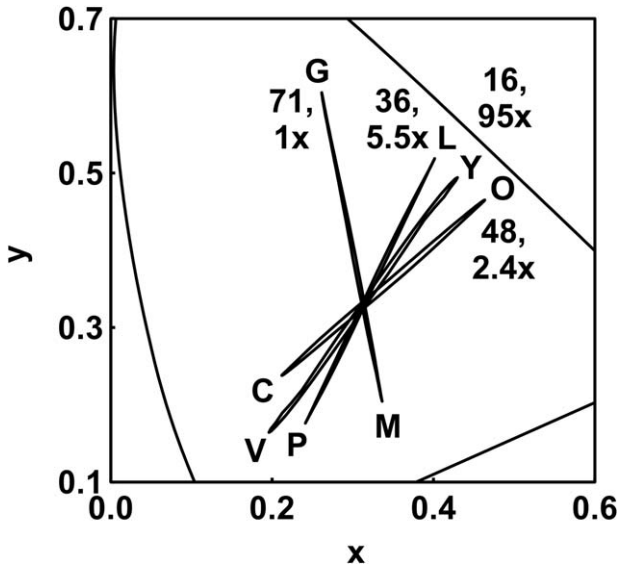

Fig. 11. Chromaticity diagram (1931) for the four cases GM ($x = 1$), OC, LP, and YV. The labeling is similar to Fig. 6.

we assigned a confidence to all of our estimates $\Delta x = \pm 0.1$, which is slightly larger than the x increment 1/12 used to construct the figure. (There is an obvious visual mismatch between these two sets of images, which is discussed below. Our complete set of images, which are not given in this report, reveal how boundary colors evolve as x and W vary, and establishes a correlation for x from 0.2 to 3.)

For example, case OC occurs in Fig. 12 at $x = 3/2$ for $W = 48$. In Fig. 4 the value 3/2 for x corresponds to the bands RYCB predicted by the appearance model, which is also seen at the left side of Fig. 12. If they are grouped as (RY)(CB) then it appears as if R and Y mix to orange and as if C and B mix to cyan.

For YV we estimated x as 5.3 for $W = 16$ based on the correspondences established in our full data set (YV and GM at $x = 5$ have similar W values), plus Fig. 4 where it corresponds to the predicted bands RYGCBM at $x = 5\frac{1}{3}$. If they are grouped as (RYG)(CBM) then it appears as if R, Y, and G mix to yellow; and, as if C, B, and M mix to violet. This is not inconceivable since we are in the realm of large dispersion shifts: small irregularities in the color-matching functions at small shifts are greatly magnified at large shifts. By "irregularities" we mean deviations from the idealized symmetries in our appearance model.

For LP we estimated x as 2 for $W = 36$ based on the right side of Fig. 12. This corresponds to KW bands in our appearance model on the left side. Regardless of this obvious model failure, we used this value of x for the LP case because it was consistent with trends in our complete data set. It is, of course, impossible to rationalize the formation of LP bands based on our appearance model. We never observed KW bands for any value of x greater than 1 in images produced from the CIE calculations, nor did we expect to find them.

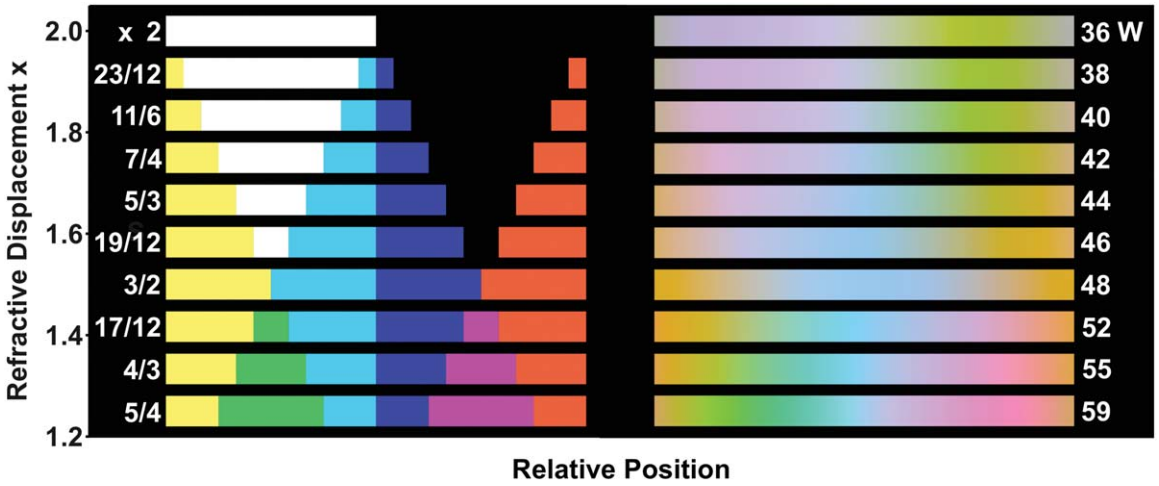

Fig. 12. At left are appearance model predictions, and at right are images for CIE calculations. Each image on the right is separately contrast enhanced. Images from the two models were correlated by visual assessment. The text explains why they differ.

KW bands recur in the appearance model because of unphysical gaps between R, G, and B image components at large dispersions. The effect of this model deficiency begins to show itself in Fig. 12 once x exceeds 3/2. Colors in the two models begin to diverge at that point in the figure. However, the divergence declines as x approaches 3, where the next member of the GM boundary colors family occurs. This pattern repeats itself as x continues to increase: the appearance model fails near x values that are even integers, and is correct near x values that are odd integers (up to $x = 7$ where such a comparison was possible).

On the right side of Fig. 12 the green and magenta bands at $x = 1.2$ (at $x = 1$ in the full data set) appear to swap places at $x = 2$. In the former case the bands are green/magenta, and at $x = 2$ they appear to be magenta/green (although we call them purple P and lime L in the case name). Note the diagonal symmetry in the right side of Fig. 12. Perhaps this observation can be used to help improve the appearance model.

Table II summarizes the correspondence between x and W for OC, LP, and YV, with the understanding that some educated guesswork was necessary (especially for LP). We are somewhat conservative specifying confidence limits for these three cases given the uncertainties for assigning x values. The next section shows that we were not unduly conservative.

APPEARANCE MODEL ACCURACY

The CIE calculation provides us with images of boundary colors that we visually experience as having appearance features that are generally unmeasurable. That is, color attributes calculated from our CIE calculations (such as CIELAB hue angle) do not usually indicate that boundary colors have visually discrete bands of color. Most current appearance models like CIECAM02 are for single colors viewed in a homogeneous surround. That being the case, how can we compare our appearance model with the colorimetric model (CIE calculation) to establish to what extent the model is accurate? Our answer is to use the data for the 7 special cases shown in Tables I and II. The special cases made it easier to assign appearance model x values to CIE calculation W values. Determining a correlation would otherwise become more subjective.

Note that x and W specify the stimulus, not the perception, although perception is necessary to establish the relationship between them. Therefore the comparison is an indirect assessment of the appearance model. The analysis that follows also does not quantify the failure of the model at even-integer values for x where black and white bands are erroneously predicted. It is probably better to say that we are testing to see if our 7 appearance model predictions are consistent with CIE calculations, ignoring other model deficiencies.

Bouma's l/r parameter provides a way to test for consistency (Ref. 1), where l is stripe width and r is the displacement due to dispersion between the shortest and longest visible wavelengths. For our appearance model l/r is inversely proportional to dispersion displacement x, and for the CIE calculation it is proportional to stripe width W. All other parameters are constant. Let us denote the former by $l/r(x)$ and the latter by $l(W)/r$. The number of wavelengths used in the CIE calculation is M - 1 and equals 300 in our case.

$$\frac{l}{r(x)} = \frac{1}{2 \cdot x} \tag{1}$$

$$\frac{l(W)}{r} = \frac{W}{M-1} \tag{2}$$

These two l/r formulas are not numerically equal. For example, the number of wavelengths used in the CIE calculation is arbitrary and this affects the value of r. The simplest assumption is that the two l/r formulas are related by a linear model, which accounts for unimportant

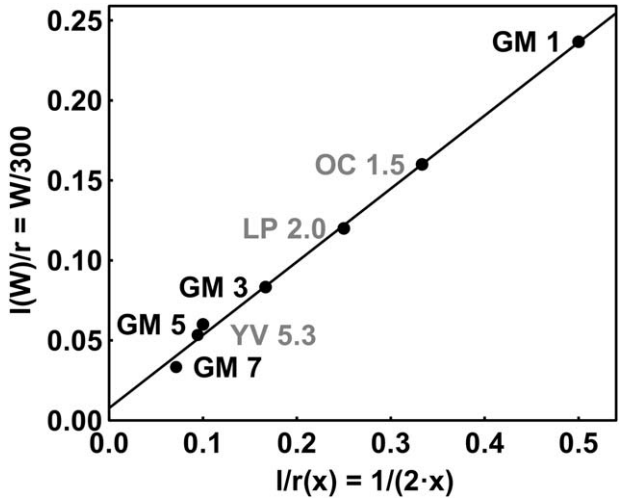

Fig. 13. Data for the 7 cases listed in Tables I and II are graphed using *l*/*r* values. The number following each case name abbreviation is the estimated *x* value. The line passing near the data points is a least squares fit. See Table III for regression results.

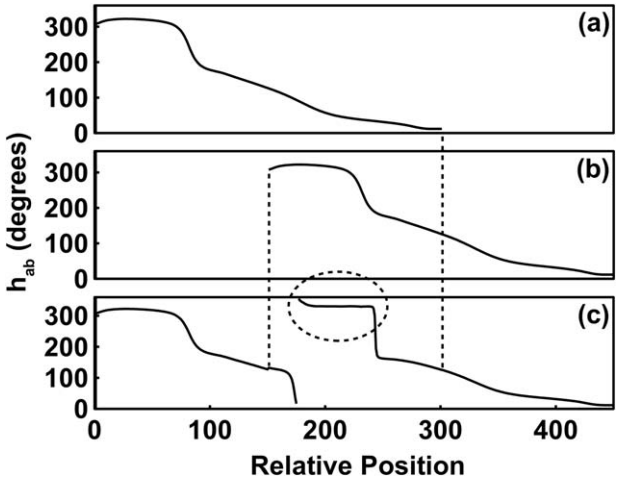

Fig. 14. (a) CIELAB hue angles for a visible spectrum, wavelengths 400 nm through 700 nm (positions 0 through 300). (b) CIELAB hue angles for a second visible spectrum, identical to the first but shifted to the right 150 units (positions 150 through 450). (c) The CIELAB hue curve when the two spectra are superimposed. The vertical dotted lines mark the range of positions where the two spectra overlap. The dotted ellipse highlights the magenta portion of the hue curve, a flat horizontal line.

offsets and differences in units. Here α and β are constants to be determined in a regression.

$$\frac{l(W)}{r} = \alpha \cdot \left(\frac{l}{r(x)}\right) + \beta \tag{3}$$

Figure 13 is a graph showing the data from Tables I and II as filled circles. A line shows the linear regression for Eq. (3). The result of the regression is shown in Table III. The standard error for predicting $l(W)/r$ equals 0.0051; it can be converted into the standard error for predicting W, which equals 1.5.

The size of the uncertainty bars for W, $\Delta W = \pm 1$, are approximately equal to the height of the filled circle symbols used for each data point in Fig. 13. The range ± 1 means that varying stripe width by 1 unit higher or lower produces a suboptimal image (less constant hues). The standard error for W in the regression, 1.5, is comparable in value to the resolution of our CIE calculations ΔW. The least squares fit in Fig. 13 passes within vertical error bars ΔW in all cases except for two: GM for $x = 5$, and GM for $x = 7$. The error bars for these two cases lie only slightly off the fitted line, so the disagreement is not very significant. In summary, scatter of the data points around the fitted line do not invalidate the linear regression model. And there are no systematic deviations from the fitted line.

TABLE III. Linear regression model.

$\frac{l(W)}{r} = \alpha \cdot \left(\frac{l}{r(x)}\right) + \beta$
$\frac{l(W)}{r} = \frac{W}{300}\frac{l}{r(x)} = \frac{1}{2 \cdot x}$
$\alpha = 0.4572\ \beta = 0.0077$
$R^2 = 0.9967$
$s_{l(W)/r} = 0.0051\ s_W = 1.5$

We expect x values associated with the GM family of boundary colors to be very certain because our appearance model is very specific about these predictions. Nonetheless the sole outliers are two GM cases. Cases OC, LP, and YV lie on the fitted line within their uncertainty bars, even though estimated x values for these cases are less confident than the GM cases because our appearance model does not explicitly predict them.

We conclude from the results of the regression that our appearance model is consistent with the CIE calculation, over a wide range of dispersions (x from 1 to 7), and over a fair range of pattern feature widths (W from 10 to 71). This is with the understanding that the appearance model fails to predict correct hues near even-integer values of x.

MAGENTA BANDS

Boundary colors predicted by our appearance model (as depicted on the left side of Fig. 12) have constant hues (and lightness) by design. We did this to model the general appearance of boundary colors as a first approximation. However, the existence of bands with constant colorimetric hue (that is, hue derived from chromaticity or CIELAB hue angle) in CIE calculations of boundary colors surprised us. The visual color matching functions are sufficiently irregular, and the wavelength composition of boundary colors are sufficiently variable, albeit smoothly varying, that we did not expect to find 7 cases with highly uniform colorimetry.

The colorimetry of boundary colors is normally smoothly varying. For example the CIELAB hue curve for the visual spectrum is fairly linear with no hint of the wide red, green, and violet bands, or the narrow yellow

and cyan bands [Fig. 14(a)]. There is greater variation in the shape of the CIELAB hue curves for other boundary colors, but we only found 7 cases where CIELAB hue exhibited well-defined plateaus, and they all occur for two-hue bands produced by repeating black and white stripe patterns. (It is possible, of course, there are other black and white patterns that produce boundary colors with constant hue bands.)

We now present what we feel is an equally surprising case where constant hue occurs, which has a bearing on boundary colors. If two visible light spectra produced by prisms or diffraction gratings are superimposed on a white screen such that the red end of one spectrum falls onto the violet end of the other spectrum, then a brilliant magenta band is perceived. It is as wide and prominent as the red, green, and violet bands in a visible spectrum.

A CIE calculation for the overlap of the two ends of spectra was adjusted to produce the most uniform magenta band. Specifically, the 600 nm wavelength of one spectrum [Fig. 14(a)] coincides with the 450 nm wavelength of the other spectrum [Fig. 14(b)], an offset of 150 nm in wavelength units. The top two curves in Fig. 14 show hue angles h_{ab} for each spectrum from 400 nm to 700 nm. Figure 14(c) shows the hue angle curve for the combined spectra (additive mixing of light). The discontinuity on the hue curve at position 176 occurs where hue crosses from 0° to 360° on the hue circle. The magenta band corresponds to the overlap of wavelength ranges 590–639 nm in Fig. 14(a) (mostly wavelengths usually perceived as orange when projected onto a white screen), and 440 nm to 489 nm in Fig. 14(b) (mostly wavelengths usually perceived as blue and cyan when projected onto a white screen).

The dashed ellipse in Fig. 14(c) encompasses the region in the overlapping spectra where hue angle is virtually constant, a flat plateau in the curve. For 50 position units (one-sixth of the 301 unit wide visible spectrum) the hue angle h_{ab} is $330.0° \pm 0.7°$. (Here, and below, the number following the $\pm$ symbol indicates a range of values around the range center. They are not measures of statistical confidence.)

This behavior for the appearance of the superposition of two visible spectra is the basis for the appearance of GM boundary colors formed by black and white stripes. This is true even though in the former case only two wavelengths comprise magenta, while in the second case many wavelengths are involved. This commonality is demonstrated by the CIELAB hue angle for the magenta boundary color in the GM case for $x = 1$, namely $330.8° \pm 0.8°$ (55 data points), which is very similar to the hue angle for the magenta band in the overlapping visible spectra, $330.0° \pm 0.7°$ (50 data points).

The overlapping visible spectra can be thought of as a special case of boundary colors. Two narrow white stripes surrounded by black can be separated by a distance such that dispersion causes two visible spectra to overlap as described. As far as we know, an analysis of the magenta band formed by superimposing two visual spectra has not been reported before.

CONCLUSIONS

Seven cases of boundary colors were discovered where colorimetric hue (such as CIELAB hue angle h_{ab}) is essentially constant for each band. The bands not only appear visually discrete, they are also colorimetrically (measurably) discrete. Normally colorimetric hue varies even when boundary color bands appear visually discrete. This more typical perception occurs for the visible spectrum. It also occurs for the simple example with two white stripes of unequal size presented early in this report, which produces 6 bands of equal widths.

The purpose of this report is not to provide a fundamental explanation for why discrete hues are generally perceived in boundary colors, or how this perception changes with viewing conditions. However, we speculate that the smooth and continuous change in boundary colors dampens the visual system's response to most image features except for red, green, and blue (or violet) color content. Our appearance model describes the perception, but does not explain it.

The trichromatic appearance model reproduces the categorical perception of 6 hues that are generally observed in boundary colors for black and white patterns, along with their band widths. Although the model is simple, it was sufficiently consistent with CIE calculations to aid our investigation. It is not obvious how to improve the model to remove prediction failures near even-integer values of x, which arise from gaps between color components that are not present in the stimulus. Even with its deficiencies and limitations, the linear regression for the 7 cases featured in this report shows that our appearance model correlates well with CIE calculations. Under the conditions that we have specified, the visual system behaves as if the cone responses are essentially independent and that the rest of the visual system is irrelevant in the perception of constant-hue bands. While certainly untrue, the assumption produces a useful model.

Someone examining the image on the left side of Fig. 12 might consider it too "cartoonish" compared with the more realistic image on the right side produced by the CIE calculation. However, if a Gaussian blur of the right amount is applied to the model "cartoon", the result is a very close match to CIE calculation images. (This assumes that accurate hues are chosen for the RGB components of the appearance model, a matter that we do not address in this report.) The orange/cyan bands for $x = 3/2$ in Fig. 12 is a case in point: a blur operation causes the red and yellow bars to blend and form orange, and the cyan and blue bars blend to form blue. Red and blue blend to form neutral band boundaries, as do cyan and yellow.

In other words, the complex CIE calculation can be replaced by our simple appearance model image followed by a blurring operation. The blur presumably accounts for the graduated cone responses that are absent from our

appearance model. We have tested blurring for complex images (including sRGB color images of natural scenes) and have obtained very satisfactory matches to the scenes observed through prisms or gratings. Blurring also ameliorates the gap problem in the model that occurs whenever $x > 1$; gaps between color components are filled by the blurring operation. Blurred appearance model predictions are always a good visual match to CIE calculation images for the repeating stripe pattern whenever $x \leq 3/2$, even when there are gaps.

We observed the green/magenta (GM) bands at $x = 1$ and the orange/blue-green (OC) bands at $x = 1.5$ using prisms and gratings. The contrast is too low to identify other cases with confidence. All images for stripe widths W smaller than about 20 units appear uniform gray in the absence of image enhancement. This corresponds to values of dispersion displacements x greater than about 4. Three of our 7 cases are in that range. However, it might be possible to confirm the hues and their uniformity for all 7 cases by using sufficiently sensitive chromaticity measurement instruments.

We believe it is relevant that supernumerary rainbows[14,15] and white light interference (Newton's rings)[16] show prominent magenta and green bands, which appear similar to the colors in the GM family of boundary colors predicted by our appearance model. A very similar magenta band is perceived by simply superimposing two visible spectra. While the physics (and therefore the colorimetry) of rainbows and light interference is well understood, our results suggest a way to better understand the appearance of these phenomena. For example, physics explains the scattering and refraction processes that form rainbows. Are there plateaus in the CIELAB hue curves of rainbows? If not, then perhaps the color bands seen in rainbows can be described using an appearance model that is similar to our model for boundary colors. One could then test whether such a rainbow appearance model also applies to the appearance of supernumerary rainbows where green and magenta bands are perceived. We feel that our appearance model opens up new possibilities for color science research.

ACKNOWLEDGEMENTS

The authors thank Mary Louise Budziak for a careful proofreading of the numerous precursors to this manuscript. Thanks too to Dr. Michael H. Brill of Datacolor for helpful discussions, suggestions, and encouragement.

1. Bouma PJ. Physical Aspects of Colour, 2nd edition. New York: St. Martin's Press; 1971. p 109–117.
2. Koenderink J. Color for the Sciences. Cambridge: The MIT Press; 2010. p 213–240.
3. McGuire JE, Tamny M. Certain Philosophical Questions: Newton's Trinity Notebook. Cambridge: Cambridge University Press; 2002. p 241, 245–249.
4. Shapiro AE. The Optical Papers of Isaac Newton, Volume I. Cambridge: Cambridge University Press; 1984. p 523–533.
5. Newton I. Opticks: Or, A Treatise of the Reflections, Refractions, Inflections and Colours of Light. The 2nd Edition, with Additions. London: WJ Innys; 1718. p 143–144.
6. Goethe JW. Zur Farbenlehre. 1810. English Translation: Eastlake CL. Goethe's Theory of Colors. London: John Murray; 1840.
7. Shepard RN. The Perceptual Organization of Colors: An Adaptation to Regularities of the Terrestrial World? Byrne A, Hilbert DR, editors. Readings on Color, Volume 2: The Science of Color. London: MIT Press; 1997. p 311–356.
8. Kidder JN. Colors of the spectrum: Do you wonder where the yellow went? Appl Opt 1994;33:4727–4732.
9. Ostwald W. Neue Forschungen zur Farbenlehre. Physikalische Zeitschrift 1916;17:322–332. English Translation: Kuehni R, Brill MH. New researches in color science. 2010. Available at: http://www.iscc.org/pdf/OstwaldFarbenlehre.pdf (August 2013).
10. Mark Fairchild, RIT Munsell Color Science Laboratory. Available at: http://www.cis.rit.edu/research/mcsl2/online/CIE/CIE2006 CMFs.xls (August 2011).
11. Hunt RWG. The Reproduction of Colour in Photography, Printing & Television, 4th edition. Tolworth, England: Fountain Press; 1987. p 4.
12. Yoder L. Relative absorption model of color vision. Color Res Appl 2005;30;252–264.
13. Color images in this article do not reproduce well in print. All images are available for viewing on calibrated color displays at http://www2.hawaii.edu/~cjenning/Faculty/Colour_Research.html (August 2013).
14. Carl Jennings, University of Hawaii at Kapiólani. Available at: http://commons.wikimedia.org/wiki/File:Supernumerary_rainbow_01_contrast.jpg (August 2013).
15. Richard Fleet, Wiltshire, England. Available at: http://www.dewbow.co.uk/bows/drop2.html (August 2013).
16. Grover Schrayer. Available at: http://www.flickr.com/photos/14833125@N02/7998465708/ in/photostream/. (August 2013).